Meteor detection for BRAMS using only the time signal

Tom Roelandts

Impulse Response, Beerse, Belgium
tom@impulseresponse.eu

Approaches for meteor detection in the BRAMS project often start from a spectrogram, since that is the default view of the received signal. In this paper, we argue that it is better to use the original time signal for detection. We define an indicator signal that consists of the ratio of received energy in a short time interval that is the length of a typical underdense meteor, and a longer time interval that represents the background signal. A simple threshold can then be used to detect underdense meteors, also in the presence of the carrier and reflections on planes.

1 Introduction

The default way to view the recorded data from the *BRAMS* (*Belgian RAdio Meteor Stations*) network (Calders and Lamy, 2012) is through a spectrogram that shows a 200 Hz range around the carrier frequency, using the *BRAMS Viewer* (Lamy et al., 2013). In this spectrogram, time is on the horizontal axis and frequency is on the vertical axis. *Figure 1* shows an example of such a spectrogram, in which several reflections are visible. The short signals with a relatively broad frequency range are *underdense* meteors, the "s-shaped" structures are *planes*, and the complicated structure near the end is an *overdense* meteor. The sampling rate is 5512 Hz, and the complete spectrogram spans a period of five minutes.

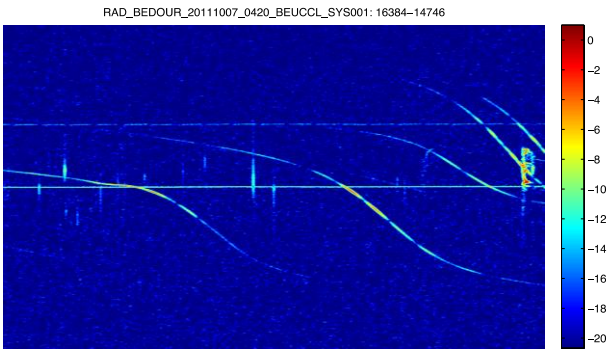

Figure 1 – Typical BRAMS spectrogram.

Since the data of the BRAMS network is viewed almost exclusively through these kinds of spectrograms, it might seem natural to attempt automatic detection of meteors also on these spectrograms, using an *image processing* approach. However, in this paper we propose a technique in which the original time signal is used directly for detection of underdense meteors. Advantages of this approach are that it is potentially faster, and that the detection parameters may have a more straightforward physical meaning as compared to an image processing approach.

The proposed method computes an *indicator signal* that has the same number of samples as the original time signal. The value of each sample of the indicator signal is the ratio of the energy in a short interval that is the length of a typical underdense meteor, and a longer interval that represents the background signal. Underdense meteors can then be detected using a simple threshold.

The remainder of this paper is structured as follows. In Section 2, the method is introduced. Section 3 describes the experiments that were performed on data of the BRAMS network. In Section 4, the results are discussed and a conclusion is reached.

2 Method

In this section, we first describe the preliminary *band-pass filter* that we apply to the time signal. We then show a straightforward, but unsuccessful, approach for detection. Finally, the indicator signal itself is introduced.

Notation

We define a discrete-time signal as a sequence of numbers $x[n]$, with $n \in \mathbb{Z}$.

Preliminary filtering

The frequencies at which the meteor reflections appear are spread around the frequency at which the carrier is received. This frequency spread is due to the Doppler effect that is caused by the intrinsic movement of the plasma trail. Since there is a physical limit to the speed of the plasma trail, there is also a certain frequency range in which the meteor reflections can be expected to appear. However, the *noise* is typically broadband, so a large part of it can be removed with a band-pass filter around the frequency of the carrier. In the experiments that follow in Section 3, we have applied a *windowed sinc* filter to implement this.

Straightforward approach

A basic observation is that underdense meteors are very short in comparison with planes and overdense meteors (see *Figure 1* for examples). If no assumptions are made on the shape of the meteor reflections, i.e., if they are considered to be short transient signals in white Gaussian noise, then *Nuttall's Maximum Detector* (Nuttall, 1997), defined as

$$x[n]_{\mathrm{NMD}} \equiv \max_m \left\{ \sum_{i=m}^{m+M-1} (x[i])^2 \right\}, \quad (1)$$

where M is the expected length of the transient, would be a very efficient way to detect them. Despite being extremely simple, this was the best performing algorithm in the review by Wang and Willett (Wang and Willett, 2000). However, it assumes that a single transient signal appears in white Gaussian noise, which is not the case here due to the reflections on planes and the fact that there are multiple meteor reflections present.

To enable detection of multiple reflections, we replace Nuttall's Maximum Detector with the running average of the signal power $(x[i])^2$, defined as

$$p_s[n] \equiv \left(\sum_{i=n-\lfloor S/2 \rfloor}^{n+\lfloor S/2 \rfloor} (x[i])^2 \right) / S, \quad (2)$$

where S (odd) is the length of the running average. This length should be chosen to be close to the typical length of an underdense meteor. In the absence of planes, a threshold could then be used to detect the meteors.

To counteract the effect of the planes, we might create a second (and much longer) running average $p_L[n]$ (defined as in (2) with L substituted for S), which could then be used to create a detection threshold that tracks the average signal power. However, practical tests have shown that the short-term fluctuations during a plane reflection are too important to allow this, and result in many false detections. This is briefly illustrated in Section 3.

The indicator signal

To define the indicator signal, we first observe that a running average of the signal power provides the mean power at every sample point. Multiplying the mean power with the length of each averaging interval provides the energy that was received over each of the intervals, i.e., $E_S[n] = Sp_S[n]$ and $E_L[n] = Lp_L[n]$.

We recall that $p_S[n]$ (and, hence, $E_S[n]$, since that is simply a multiple of $p_S[n]$) would be expected to be a very good detector if the meteors were embedded in white noise, due to its similarity to Nuttall's Maximum Detector, as detailed in the previous section. However, they are not expected to work for the BRAMS data, due to the disturbances that are caused by the planes.

The indicator signal compensates for the plane reflections by comparing the received energy in a short time interval with the energy in a much larger surrounding interval. It is defined as

$$I[n] \equiv \frac{E_S[n]}{E_L[n]}. \quad (3)$$

Since each sample of $I[n]$ has $E_L[n]$ in the denominator, a very small value $E_L[n]$ might cause relatively high values for $I[n]$, even though $E_S[n] \leq E_L[n]$ always. Hence, to avoid false detections, we limit the value of $E_L[n]$ to some small value in the experiments of Section 3.

Meteor detection

The detection of the meteors is then trivial. A fixed threshold is chosen, and a meteor starts when the indicator signal rises above the threshold and stops when it drops under the threshold again.

3 Experiments and results

The experiments were based on data from the BRAMS project. For all datasets, a band-pass filter of width 60 Hz centered on the carrier was applied, and the values $S = 101$ and $L = 30001$ were used. Note that these values depend on the sampling rate and cannot be used directly for other systems.

The first experiment, for which we provide detailed results, was recorded with the Uccle receiving station. This is the data set of which the example spectrogram in Section 1 was made (*Figure 1*).

We now illustrate that the preliminary filtering that was introduced in Section 2 clearly improves the detectability of the meteor reflections. The reflections are not visible as clear peaks in the original time signal (*Figure 2*) or in the signal power (*Figure 3*). After band-pass filtering (*Figure 4*), the detectability of the meteors has clearly improved. The corresponding spectrogram of the filtered signal is shown in *Figure 5*. However, the signal strength that is generated by the reflections on some of the planes is of the same magnitude as those of the smaller meteors, making it impossible to discriminate between them using a simple threshold.

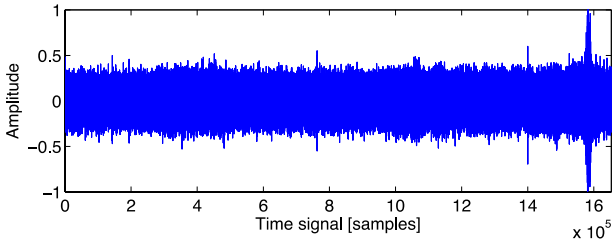

Figure 2 – Amplitude of original signal.

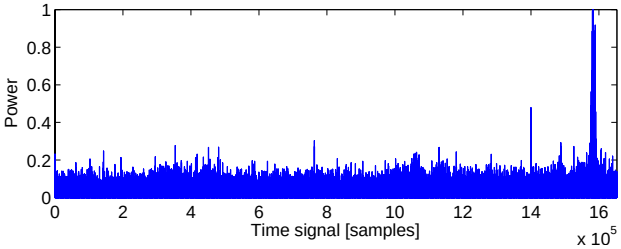

Figure 3 – Power of original signal.

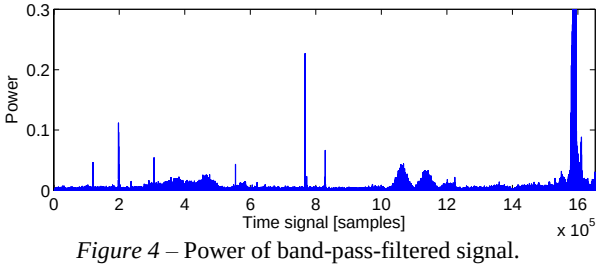

Figure 4 – Power of band-pass-filtered signal.

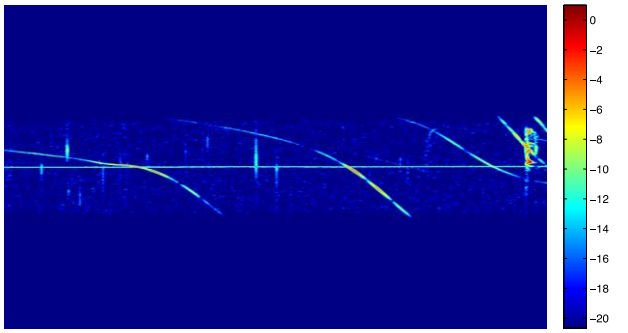

Figure 5 – Band-pass-filtered spectrogram.

The straightforward approach with running averages of Section 2 is illustrated in *Figure 6*. The blue curve is a running average of length S. The red curve is a running average of length L that has been offset by a certain amount, i.e., a constant has been added, to form a threshold. Even when, in this example, the threshold is too high to detect the smaller meteor reflections, it already touches the plane reflections, which would result in false detections. This shows that the approach with simple running averages cannot be expected to work in practice.

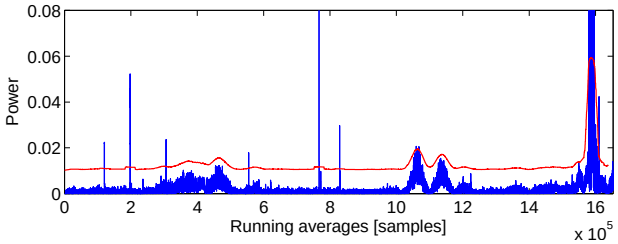

Figure 6 – Running averages of (blue) 101 samples and (red) 30001 samples.

The indicator signal for this data set is shown in *Figure 7*. The "bulges" that were caused by the plane reflections in *Figure 4* have disappeared. This allows using a simple constant threshold, as indicated by the red line in *Figure 7*. The spectrogram of *Figure 1* is shown again in *Figure 8*, with added red dots that indicate where meteors were detected.

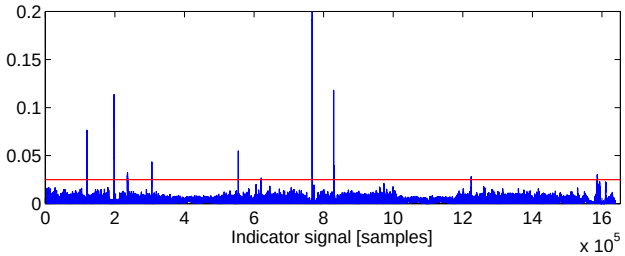

Figure 7 – Indicator signal (blue) and detection threshold (red).

We now show, for three other datasets, the indicator signal and the corresponding spectrogram with added red dots that indicate where meteors were detected. We reiterate that these experiments were run using the exact same set of parameters. This does not imply that these parameters should never be adapted to the data at hand, but it does imply that the parameters do not have to be tuned for each specific data set.

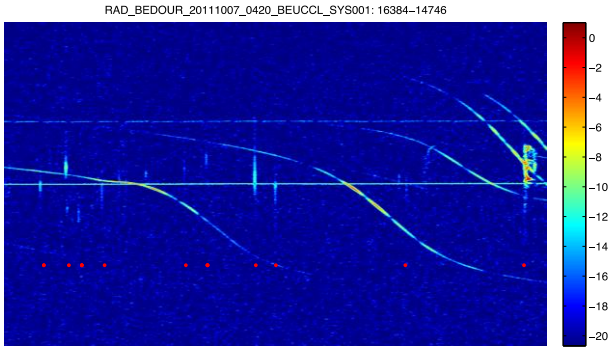

Figure 8 – Spectrogram with detected meteors.

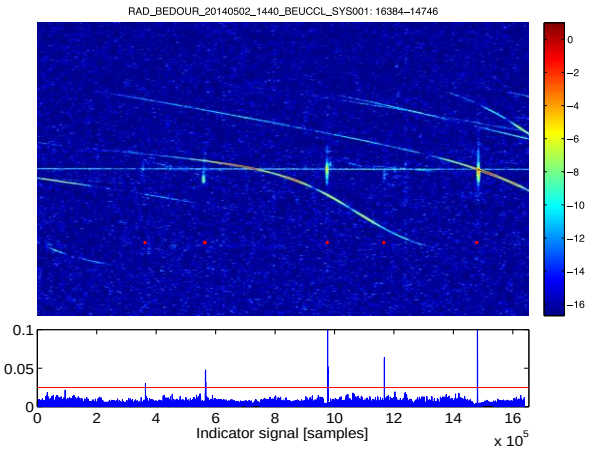

Figure 9 – Detected meteors and indicator signal.

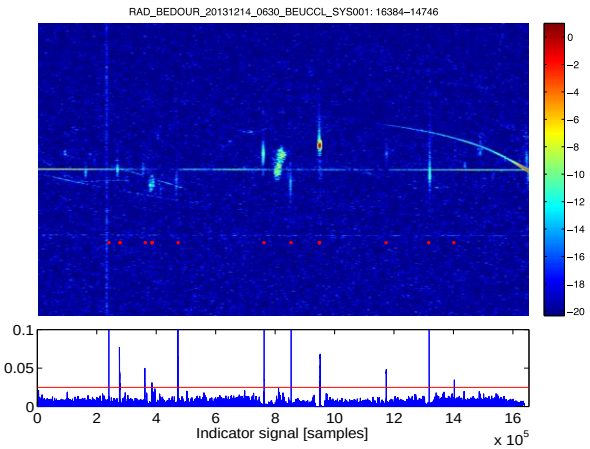

Figure 10 – Detected meteors and indicator signal for a spectrogram containing a wideband pulse.

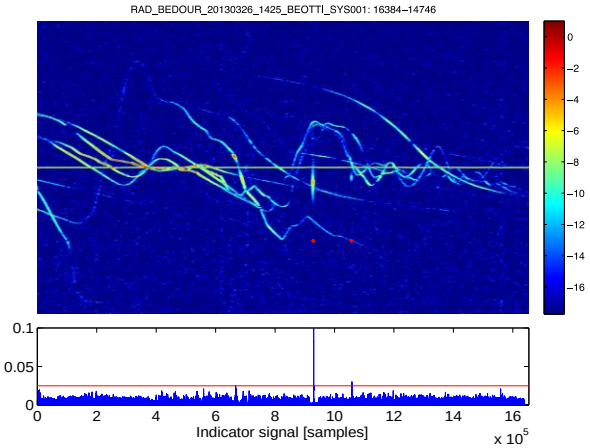

Figure 11 – Detected meteors and indicator signal for a spectrogram with many planes.

Figure 9 is a clean example with some planes and some underdense meteors that are all detected correctly. The

spectrogram of *Figure 10* contains a wideband pulse. Since the pulse is short, it is detected as a meteor. This means that it is necessary to check for these kinds of pulses separately and reject them. One way to do this is check (for each potential meteor) whether it can also be detected outside of the normal frequency range. This would indicate that it is too wideband to be a meteor. In *Figure 11*, many planes are present, and they seem to be performing more complicated maneuvers than usual. However, this does not hamper the detection of the meteors.

4 Discussion and conclusion

Much of the research that is done towards detection of meteors in systems such as the BRAMS network is concentrated on image processing techniques that operate on the spectrogram. With this paper, we have tried to present an alternative method that uses the time signal directly. And, even though the presented indicator signal should be considered a preliminary result, it does show that this is possible.

For future work, we intend to study a *matched filter* approach, where the expected shape of the meteor reflection, i.e., a sudden rise followed by an exponential decay, is matched directly through correlation. The current solution amounts to correlation with a rectangular pulse, which is not the at all like the true shape of the reflection. Another possibility is that the indicator signal can possibly also provide a confidence level for each meteor detection, since it indicates exactly which fraction of the energy is concentrated in the central peak. It might also be beneficial to repeat the detection process several times with different lengths for the long and short intervals, to detect shorter and longer meteors separately.

In conclusion, we have introduced an indicator signal based on the time signal, which can be used to detect underdense meteors using a simple threshold, for systems such as the BRAMS network.

A Python implementation of the indicator signal is available on the website of the author[1].

References

Calders S. and Lamy H. (2012). "Brams : status of the network and preliminary results". In Gyssens M. and Roggemans P., editors, *Proceedings of the International Meteor Conference*, Sibiu, Romania, 15–18 September 2011. IMO, pages 73–76.

Lamy H., Gamby E., Ranvier S., Geunes Y., Calders S., and De Keyser J. (2013). "The BRAMS Viewer: an on-line tool to access the BRAMS data". In Gyssens M. and Roggemans P., editors, *Proceedings of the International Meteor Conference*, La Palma, Canary Islands, Spain, 20–23 September 2012. IMO, pages 48–50.

Nuttall A. H. (1997). Detection capability of linear-and-power processor for random burst signals of unknown location. Naval Undersea Warfare Center Division.

Wang Z. and Willett P. (2000). "A performance study of some transient detectors". *IEEE Trans. Image Process.*, **48**, 2682–2685.

[1] http://tomroelandts.com/articles/meteor-detection-for-brams-using-only-the-time-signal.